



JAEA-Review

2006-009



JP0650294

Review of JAEA Activities on the IFMIF Liquid Lithium Target in FY2005

Mizuho IDA, Hiroo NAKAMURA

Teruo CHIDA and Masayoshi SUGIMOTO

Fusion Materials Development Group
Fusion Research and Development Directorate

March 2006

Japan Atomic Energy Agency

日本原子力研究開発機構

JAEA-Review

本レポートは日本原子力研究開発機構が不定期に刊行している研究開発報告書です。
本レポートの全部または一部を複写・複製・転載する場合は下記にお問い合わせ下さい。

〒319-1195 茨城県那珂郡東海村白方白根2-4

日本原子力研究開発機構 研究技術情報部 研究技術情報課

Tel.029-282-6387, Fax.029-282-5920

This report was issued subject to the copyright of Japan Atomic Energy Agency.
Inquiries about the copyright and reproduction should be addressed to :

Intellectual Resources Section,

Intellectual Resources Department

2-4, Shirakata-shirane, Tokai-mura, Naka-gun, Ibaraki-ken, 319-1195, JAPAN

Tel.029-282-6387, Fax.029-282-5920

©日本原子力研究開発機構, Japan Atomic Energy Agency, 2006

Review of JAEA Activities on the IFMIF Liquid Lithium Target in FY2005

Mizuho IDA[※], Hiroo NAKAMURA, Teruo CHIDA[※] and Masayoshi SUGIMOTO

Division of Fusion Energy Technology
Fusion Research and Development Directorate
Japan Atomic Energy Agency
Naka-shi, Ibaraki-ken

(Received January 27, 2006)

The International Fusion Materials Irradiation Facility (IFMIF) is being jointly planned to provide an accelerator-based Deuterium-Lithium (D-Li) neutron source to produce intense high energy neutrons (2 MW/m^2) up to 200 dpa and a sufficient irradiation volume (500 cm^3) for testing candidate materials and components up to about a full lifetime of their anticipated use in ITER and DEMO. To realize such a condition, 40 MeV deuteron beam with a current of 250 mA is injected into high speed liquid Li flow with a speed of 20 m/s. In target system, radioactive species such as ^7Be , tritium and activated corrosion products are generated. In addition, back wall operates under severe conditions of neutron irradiation damage (about 50 dpa/y). In this paper, the thermal structural analysis and the accessibility evaluation of the IFMIF Li loop are summarized as JAEA activities on the IFMIF target system performed in FY2005.

Keywords: IFMIF, Target Assembly, Nuclear Heating, Thermal Stress, Beryllium-7, Worker Dose

※ Cooperative Staff

IFMIF 液体リチウムターゲットに関する平成 17 年度の原子力機構の活動

日本原子力研究開発機構核融合研究開発部門

核融合エネルギー工学研究開発ユニット

井田 瑞穂*・中村 博雄・千田 輝夫*・杉本 昌義

(2006 年 1 月 27 日受理)

国際核融合材料照射施設(IFMIF)は、核融合炉材料の開発のために、十分な照射体積(500 cm³)を有し照射量200 dpaまで照射可能な強力中性子束(2 MW/m²)を発生可能な加速器型中性子源である。このような中性子を発生させるために、最大エネルギー40 MeV、最大電流250 mAの重水素ビームを、最大流速20 m/sの液体リチウム流ターゲットに入射させる。ターゲット系では、ベリリウム-7、トリチウムや放射化腐食生成物等が発生する。また、背面壁は、年間50 dpaの中性子照射下で使用する必要がある。本報告では、平成17年度の原子力機構におけるターゲット系の活動での主要なトピックスとして、核発熱条件下でのターゲットアセンブリの熱構造解析、ベリリウム-7によるリチウムループ近接性の影響評価を取りまとめた。

Contents

1. Introduction	1
Reference	1
2. IFMIF Liquid Lithium Target	2
2.1 Target Facility	2
2.2 Target Assembly	2
2.3 Lithium Loop	3
References	3
3. Thermo-structural Analysis of Back-wall	7
3.1 Introduction	7
3.2 Calculation Model and Conditions	7
3.3 Results and Discussions	8
3.4 Future Data Need	9
3.5 Summary	9
References	10
4. Radiation Dose Rate Due to Beryllium-7	21
4.1 Calculation Condition	21
4.2 Results	22
4.3 Summary	25
References	25
5. Summary	26
Acknowledgements	26
Appendixes	27

目次

1. はじめに	1
参考文献	1
2. IFMIF 液体リチウムターゲット	2
2.1 ターゲット系	2
2.2 ターゲットアセンブリ	2
2.3 リチウムループ	3
参考文献	3
3. 背面壁の熱応力解析	7
3.1 はじめに	7
3.2 計算モデルと計算条件	7
3.3 結果と考察	8
3.4 今後のデータ要求	9
3.5 まとめ	9
参考文献	10
4. ベリリウム-7による照射線量率	21
4.1 計算条件	21
4.2 結果	22
4.3 まとめ	25
参考文献	25
5. まとめ	26
謝辞	26
付録	27

1. Introduction

The International Fusion Materials Irradiation Facility (IFMIF) is an accelerator-based deuterium-lithium (D-Li) neutron source for testing the effects of neutron irradiation on the properties of candidate materials of fusion reactors. The IFMIF activity has been implemented since 1995 as an international collaboration under auspice of the International Energy Agency (IEA), and IFMIF design at 2003 was identified in IFMIF Comprehensive Design Report (CDR) [1.1]. The IFMIF activity is still under going as that in a transition phase to IFMIF Engineering Validation and Engineering Design Activity (EVEDA).

To provide the intense neutron flux of 4.5×10^{17} neutrons/m²/s with a peak energy around 14 MeV, two deuterium beams with total current of 250 mA and energy of 40 MeV are injected into a flowing liquid lithium target, which is operated at maximum flow speed up to 20 m/s for removal of 10 MW heat deposition by the deuterium beams and suppression of the excessive increase of lithium temperature.

Stability of this high-speed free-surface lithium flow is a key issue to assure quality of the neutron flux and integrity of the target facility. Thermal stress in and deformation of the target assembly are caused by nuclear heating due to the neutrons in the IFMIF operation. Since they affect respectively the target integrity and the flow stability, thermal stress analysis was performed using a calculation code and material data. Furthermore, stability of free-surface flow without beam injection was experimentally examined using a small lithium loop.

Impurity in the liquid lithium is a key issue to assure long-term integrity of the target facility and worker safety at maintenance. Effect of beryllium-7 upon worker dose was estimated using a calculation code, since its radioactivity is the most dominant among nuclides in the lithium loop. Removals of nitrogen and hydrogen isotopes from liquid lithium were examined using elemental setup including candidate materials for impurity trapping.

This report consists of the activities in FY2005 above mentioned. The analyses were performed by Japan Atomic Energy Research Institute (JAERI) until September 2005 and by Japan Atomic Energy Agency (JAEA) after merger with Japan Nuclear Cycle Development Institute (JNC) in October 2005.

Reference

- [1.1] IFMIF International Team, "IFMIF Comprehensive Design Report", IEA on-line publication, http://www.iea.org/Textbase/techno/technologies/fusion/IFMIF-CDR_partA.pdf and partB.pdf

2. IFMIF Liquid Lithium Target

2.1 Target Facility

The IFMIF consists of the accelerator facility, the target facility and the test facilities. Features of IFMIF target are a lithium target for simulating fusion neutrons with energy peak around 14 MeV through D-Li reaction, and a liquid target for removal of heat locally deposited with high density inevitable at the high-flux neutron generation.

Three-dimensional arrangement of the target facility is shown in Fig. 2-1. Two deuteron beams with total current of 250 mA and energy of 40 MeV are injected into a rectangular foot-print of ${}^H50\text{ mm} \times {}^W200\text{ mm}$ on the lithium target. To remove this high heat load with density of 1 GW/m^2 , the lithium target flows with flow velocity up to 20 m/s in the target assembly. The total heat load of 10MW is removed through the primary lithium loop, the secondary organic-oil loop and the tertiary water loop. The primary lithium loop consists of a main loop with flow rate of 130 liter/s and a purification loop with impurity traps. Major design requirements are summarized in Table 2-1.

2.2 Target Assembly

Three-dimensional view of the target assembly is shown in Fig. 2-2. The target assembly with weight of about 600 kg is supported and adjusted by the support attached to both side walls of a Test Cell room under a condition of vacuum ($1 \times 10^{-3}\text{ Pa}$) or filled with Ar/He gas. The target assembly made of stainless steel 316 has lip seals (indicated in blue) for welding/cutting by yttrium aluminum garnet (YAG) laser. Considering high irradiation damage up to 50 dpa/year, the back-wall is made of 316-steel or reduced-activation ferritic/martensitic (RAFM) and replaced after every 11-months operation. There are two options for the replaceable back-wall. One is a back-wall with lip seal welding/cutting as shown in Fig. 2-1. The other is a “bayonet type” back-wall with mechanical slide-guide and bolting. In the JAEA activity, the former type has been examined from viewpoint of thermal stress and deformation due to nuclear heating by neutrons during an operation.

Cross-sectional view of the target assembly is shown in Fig. 2-3. The liquid lithium with width of 260 mm flows down, with reducing its thickness from 250 mm to 25 mm and increasing its flow velocity up to 20 m/s in the double reducer nozzle, then along the concave back-wall with radius of 250 mm to avoid lithium boiling by a centrifugal force in the free-surface flow under the accelerator vacuum condition of $1 \times 10^{-3}\text{ Pa}$. Surface behaviors of high-speed free-surface flow generated by a smaller double reducer nozzle have been experimentally examined under JAEA/Osaka University collaboration.

2.3 Lithium Loop

The function of the main lithium loop is removal of the heat up to 10 MW. As shown in Fig. 2-1, the main loop consists of an electro magnetic pump (EMP) to circulate the liquid lithium, the target assembly to form the liquid target, a quench tank to relax lithium temperature distribution localized due to the beam injection, a heat exchanger (HX) to cool the liquid lithium, and a dump tank to storage the lithium with inventory of 9 m³. All components are made of 316 steel, excepting a RAFM back-wall.

In the lithium loop, radioactive nuclides are produced through nuclear reaction between deuteron/neutron and lithium/steel elements. Radioactivity of corrosion products from an activated back-wall after 1 year operation was estimated 4×10^{10} Bq in FY2004.[2.1] Radioactivity of tritium remaining in the lithium loop was estimated 6×10^{14} Bq also in FY2004.[2.2] In comparison with them, radioactivity of beryllium-7 (⁷Be) produced through ⁶Li(D, n)⁷Be and ⁷Li(D, 2n)⁷Be is larger (estimated 5×10^{15} Bq). Furthermore, a nuclide ⁷Be decays emitting a gamma ray with high energy of 0.48 MeV, and sufficient reduction of the radioactivity within 1-month annual maintenance, since half-life of ⁷Be is 53.3 days. Therefore, ⁷Be is the most dominant nuclide from viewpoint of worker dose. Effects of these radioactive nuclides have been estimated as JAEA activity.

Most of impurities including radioactive ones in liquid lithium are expected to be removed in the cold/hot traps in the lithium purification loop. Required concentration of each element is less than 10 wppm. Hydrogen isotopes are trapped mainly in the hydrogen hot trap with yttrium (Y) sponge operated at 285 °C. Nitrogen are trapped mainly in the nitrogen hot trap operated at 550-600 °C. Candidate materials for the nitrogen hot trap are vanadium titanium (V-Ti) alloy and zirconium (Zr).

References

- [2.1] H. Nakamura, M. Takemura, M. Yamauchi, U. Fischer, M. Ida, S. Mori, T. Nishitani, S. Simakov and M. Sugimoto, "Accessibility Evaluation of the IFMIF Liquid Lithium Loop Considering Activated Erosion/Corrosion Materials Deposition", *Fusion Eng Des* 75-79 (2005) 1169-1172.
- [2.2] K. Matsuhiro, Hirofumi Nakamura, T. Hayashi, Hiroo Nakamura and M. Sugimoto, "Evaluation of Tritium Permeation from Lithium Loop of IFMIF Target System", *Fusion Science and Technology* 48 (2005) 625-628.

Table 2-1. Major design requirements of IFMIF target facility.

Items	Parameters
Deuteron energy	40 MeV
Deuteron beam current	125 mA x 2 accelerators
Beam footprint on Li flow	^H 50 mm x ^W 200 mm
Beam power, heat flux	10 MW, 1 GW/m ²
Li flow thickness (inc. deviation), width	^T 25±1 mm, ^W 260 mm
Li flow average velocity	15 m/s (range: 10-20 m/s)
Li flow rate in main loop	0.13 m ³ /s (at 20 m/s)
Nozzle geometry	Double reducer based on Shima's model
Nozzle contraction ratio	10 → 2.5 → 1 (^T 250 → 62.5 → 25 mm)
Surface roughness of nozzle inner wall	< 6 μm
Li temperature at inlet	250 °C (nominal)
Vacuum condition at Li free surface	10 ⁻³ Pa
Vacuum, filling gas in Test Cell room	0.1 Pa, ~0.1 MPa-Ar/He (TBD)
Hydrogen isotopes concentration in Li	< 10 wppm (total of ¹ H, ² H, ³ H), < 1 wppm (³ H)
Impurity concentration in Li	< 10 wppm (each C, N, O)
Corrosion concentration in Li	TBD
Erosion/corrosion rate	< 1 μm/year (back-wall, nozzle) < 50 μm/30year (others)
Component material	RAF or 316 steel (back-wall) 316 steel (others, excepting impurity-getter materials)
Replacement period	Every 11-months operation (back-wall) No replacement in 30 years (others)
Alignment accuracy of back-wall	±0.5 mm
Availability of target facility	> 95 %

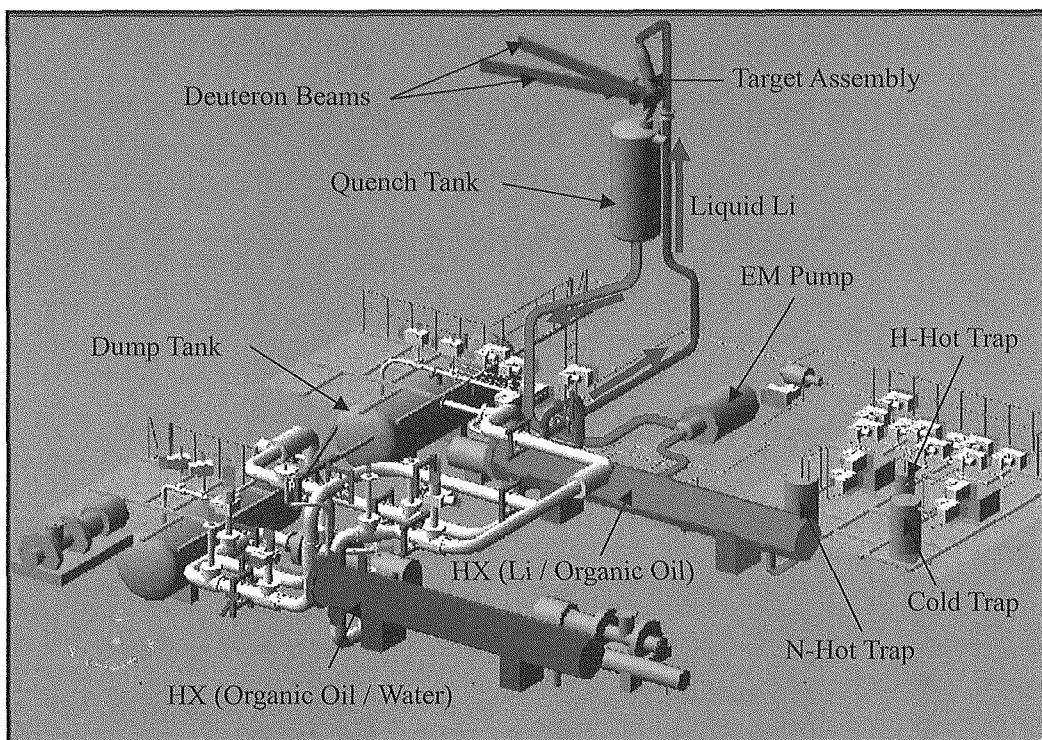


Fig. 2-1 Three-dimensional arrangement of the IFMIF target facility.

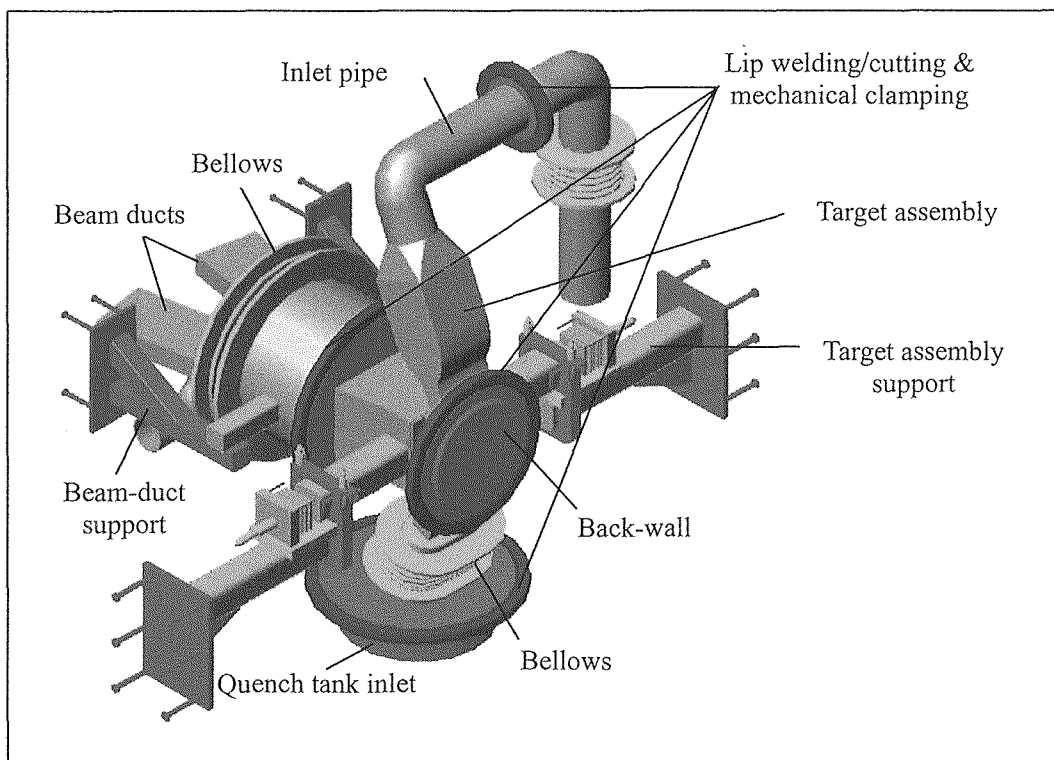


Fig. 2-2 Three-dimensional view of the IFMIF target assembly.

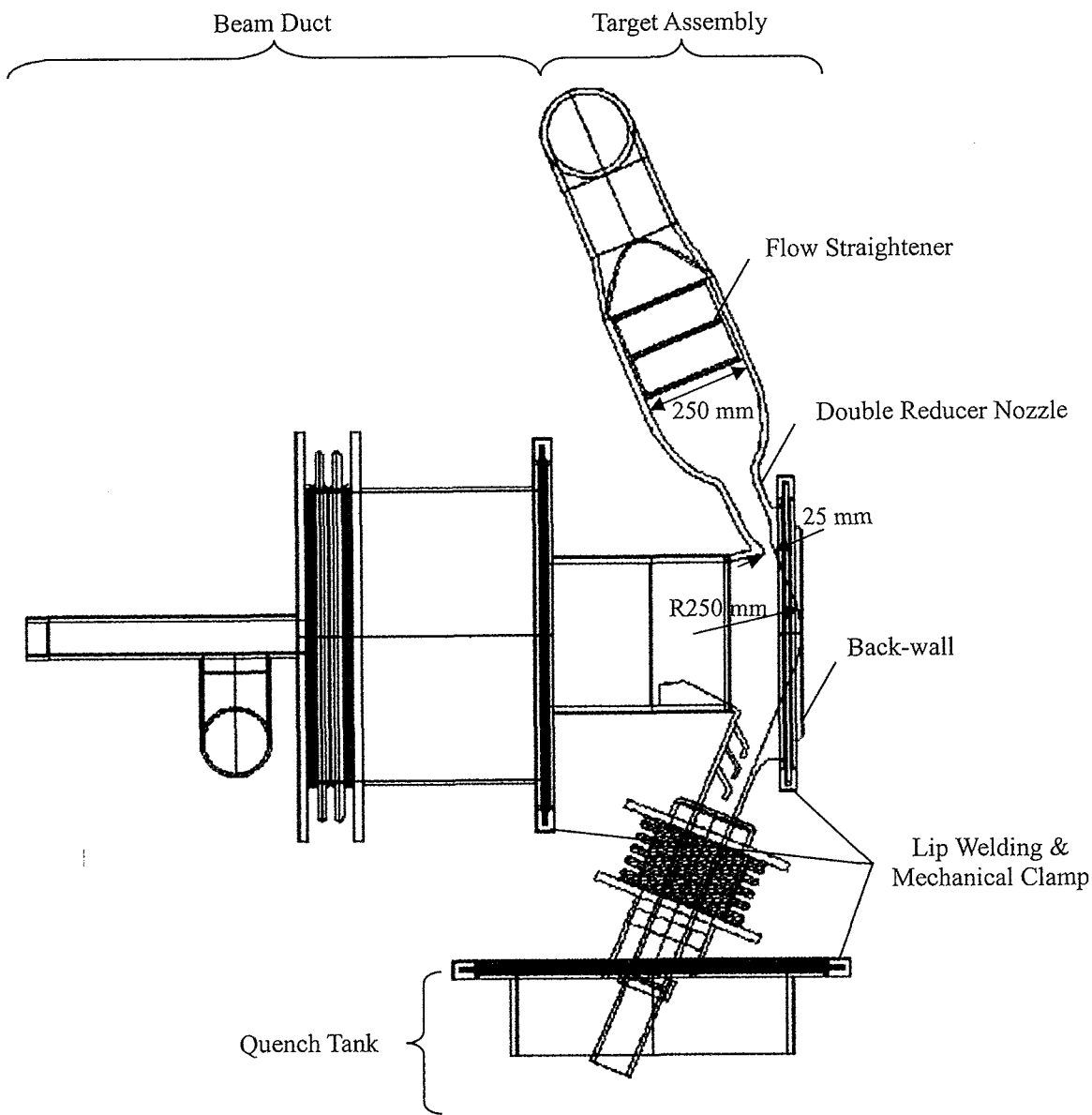


Fig. 2-3 Cross-section of IFMIF target assembly.

3. Thermo-structural Analysis of Back-wall

3.1 Introduction

In the IFMIF, intense neutrons are emitted inside the Li flow through a thin back-wall attached to the target assembly [3-1]. Since the back-wall is operating under a severe neutron irradiation of 50 dpa/year and a maximum nuclear heating rate of 25 W/cm^3 , thermo-structural design is one of critical issues in a target design. The back-wall is designed for replacement every 11 months. The target assembly is stainless steel alloy except for the back-wall made of 316L stainless steel or Reduced-Activation Ferritic/Martensitic (RAFM) steel such as F82H. In a previous study [3-2], [3-3], thermal stress analysis of the 316 stainless steel back-wall has been done to evaluate dependences of a constraint condition and a thermal transfer coefficient on the thermal stress. Two design options of the back-wall replacement are under investigation. The first option is called the “Cut and reweld” option shown in Fig.3-1. The back-wall is connected to the target assembly by welded lip seal and a mechanical clamp at the circumference. For replacement of the back-wall itself, the overall target assembly with the back-wall is removed using a remote handling system to the hot cell area where YAG laser device will be used for cutting the lip seals of the flanges. The second option is called the “bayonet” option shown in Fig.3-2. In this case, “bayonet” type mechanical attachment of the back-wall to the target assembly is envisaged. To replace the back-wall of the target assembly, a remote handling device is used in a test cell room [3-4].

In this section, the latest results of the thermo-structural design of the “Cut and reweld” back-wall option has been described.

3.2 Calculation Model and Conditions

Deformation and thermal stress of the back-wall due to nuclear heating by neutron irradiation was estimated by using ABAQUS code [3-5]. Figure 3-3 shows calculation model of the back-wall. Its shape is nearly a disc with a diameter of 0.715 m. Its Li flow side has a concave face with a radius of 0.25 m. The analysis was performed for 1/4 section ($0 \text{ m} < Y, 0 \text{ m} < Z$) of the back-wall because of its symmetry. Distribution of nuclear heating rate is shown in Fig.3-4 [3-6]. The maximum value of the nuclear heating rate was 25 W/cm^3 at beam center ($Y = 0 \text{ m}, Z = 0 \text{ m}$). In previous study, two cases for the boundary condition were considered at the circumference of the back-wall. One is constraint for all degrees of freedom, and the other is that only in X direction. Since the former constraint is not acceptable due to high thermal stress, the latter constraint is used in this analysis. Temperatures of the target assembly and liquid Li were both $300 \text{ }^\circ\text{C}$, and thermal transfer coefficient between Li and the back-wall was $34 \text{ kW/m}^2\cdot\text{K}$ that was estimated as the minimum value from experimental results [3-7]. Emissivity of the back-wall was 0.3. Temperature of vertical test assembly (VTA) is assumed to be $50 \text{ }^\circ\text{C}$ because an effect of the VTA temperature from $50 \text{ }^\circ\text{C}$ to $150 \text{ }^\circ\text{C}$ on the back-wall temperature was found to be negligible.

Thermal transfer coefficients between the back-wall and the target assembly were 15.8, 79 and $158 \text{ W/m}^2\cdot\text{K}$ depending on the contact pressure due to clamping mechanism, which was assumed to be 0.1,

0.5 and 1 MPa, respectively. To evaluate effects of the back-wall thickness on the thermal stress and the deformation, the minimum thickness of the back-wall was selected to be 1.8 (reference value), 3 and 5 mm. In the back-wall, an inelastic deformation of the back-wall is not allowed to realize a stable high speed Li flow. Therefore, a permissible stress of the back-wall is defined by yield strength. In addition, the yield strength of unirradiated condition was used because the yield strength increases after neutron irradiation. The permissible stresses of 316L [3-8] and F82H [3-9] are shown in Figs.3-5 and 3-6. To prevent from deterioration of high-speed Li flow, the deformation of the back-wall needs to be as small as possible. Permissible deformation value will be defined by a future study on Li flow stability.

3.3 Results and Discussions

3.3.1 Thickness and Thermal Transfer Coefficient

In the previous analysis of the 316L stainless steel back-wall with a minimum thickness of 1.8 mm and a thermal transfer coefficient of $158 \text{ W/m}^2\cdot\text{K}$ between the target assembly body and the back-wall, the maximum thermal stress and deformation at a center of the back-wall were about 260 MPa and 0.3 mm, respectively [3-3]. Temperature at a center of the back-wall was about 300 °C close to Li temperature. The calculated thermal stress was beyond a permissible value of 164 MPa at 300 °C for 316L stainless steel. Although the permissible deformation value is not yet defined, to mitigate the thermal stress and the deformation, an effect of the minimum thickness (t_{\min}) of the back-wall and the thermal transfer coefficient on the thermal stress and the deformation was evaluated. Results with $t_{\min} = 1.8 \text{ mm}$ and thermal transfer coefficient (α) $15.8 \text{ W/m}^2\cdot\text{K}$ are shown in Figs.3-7 and 3-8. Dependence of the minimum thickness on the thermal stress and the deformation are shown in Fig.3-9. Increasing the minimum thickness of the back-wall, the thermal stresses decrease and are close to constant values. However, in a range of 15.8 to $158 \text{ W/m}^2\cdot\text{K}$, which corresponds to a contact pressure of 0.1 to 1 MPa, the induced thermal stresses are still above the permissible value even in 5 mm case. Considering realistic design conditions on the thermal transfer coefficient and the minimum back-wall thickness, 316L stainless steel is not recommended as the back-wall material in the IFMIF.

3.3.2 Back-wall Material

Considering advantages of reduced radioactivity and higher mechanical strength than 316L stainless steel, Reduced-Activation Ferritic/Martensitic (RAFM) steel such as F82H was selected as a candidate material. Using the reference configuration with a minimum thickness of 1.8 mm, thermal stress analyses have been done. Figures 3-10 and 3-11 show contour of the temperature and the von Mises stress of the F82H back-wall, respectively. High thermal stresses are observed at a center and a corner of the back-wall. Figure 3-12 shows the von Mises stress and the deformation as a function of the thermal transfer coefficient between the back-wall and the target assembly. For a comparison, results of the 316L back-wall are also shown. According to IEA data base [3-9], a permissible stress defined by yield strength of F82H is

455 MPa at 300 °C. Even in the case of reference condition (15.8 W/m²·K), the von Mises stress is below the permissible value. The deformation of the F82H back-wall is 0.3 to 1.1 mm in a range of the thermal transfer coefficient (15.8 to 158 W/m²·K). From a viewpoint of the thermo structural design, F82H is recommended as a back-wall material

3.3.3 Revised Model

In the previous sections, the thermo-structural analysis of the back-wall was performed independent of the target assembly. However, the constraint condition with a freedom to radial direction needs to be evaluated in more detail. Therefore, a model with a simplified target assembly was applied. In this model, to simulate the target assembly, a thick plate with a thickness of 30 mm was added behind the back-wall. The plate with a lip seal was connected to the back-wall lip seal. As the results, induced thermal stresses at the back-wall center and the lip seal are beyond the permissible values. To mitigate the thermal stress and deformation at the back-wall center, modification of the lip seal configuration was applied. Calculation model is shown in Fig.3-13. In the lip seal, semi-circular part is added to mitigate thermal expansion. Typical results are shown in Figs. 3-14, 3-15 and 3-16. As the results, the thermal stress and the deformation at the back-wall center are reduced to 60-90 MPa and about 0.1 mm, respectively. In this case, the maximum thermal stress is observed at the lip seal. These results show that the modification of the lip seal with a round part is effective to reduce the thermal stress and the deformation.

3.4 Future Data Need

To apply F82H to the back-wall, one of design issues is lip seal welding between the F82H back-wall and the 316L stainless steel target assembly because a welding between F82H and 316L stainless steel is difficult. To solve this issue, use of an interlayer between the target assembly lip and the back-wall lip will be evaluated. R&D on the lip seal welding including the interlayer is planned. In the reference configuration of the “Cut and reweld” back-wall, neutron irradiation at the lip seal location in full performance of the IFMIF is estimated to be 0.1 to 1 dpa/y although neutron irradiation at a center of the back-wall is 50 dpa/y. In this condition, He generation rate is about 1 to 10 appm. Rewelding characteristics of the irradiated lip seal needs to be evaluated. To mitigate the deformation of the back-wall, optimization of the back-wall configuration is under investigation. Moreover, further study on a constraint condition of the back-wall is under way.

In a next phase of IFMIF project called as EVEDA, engineering design and validation on the replaceable back-wall will be performed.

3.5 Summary

Thermo-structural analyses of the “Cut and reweld” type replaceable back-wall made of 316L stainless steel and F82H have been done by ABAQUS code. In a case of the 316 stainless steel back-wall, the von Mises stress was higher than a permissible value of 140 MPa at 300 °C. However, in a case of F82H back-wall, the von Mises stress is less than a permissible value of 455 MPa at 300 °C. Therefore,

F82H is recommended as a back-wall material. In case of the revised model with a simplified target assembly and the lip seal, the thermal stress and the deformation at the back-wall center are significantly reduced. But, in this case, the maximum thermal stress is observed at the lip seal.

In future, engineering design and validation of the target system will be done in the EVEDA.

References

- [3-1] H. Nakamura et al., Fusion Eng. and Des. 66-68 (2003) 193.
- [3-2] M. Ida, et al., Fusion Eng. and Des. 75-79 (2005) 847.
- [3-3] H. Nakamura, et al., “Review of JAERI Activities on the IFMIF Liquid Lithium Target in FY2004”, JAERI Report, JAERI-Review 2005-005 (2005).
- [3-4] B. Riccardi, et al., Fusion Eng. and Des. 66-68 (2003) 187.
- [3-5] Hibbitt, Karlsson & Sorensen, Inc., ABAQUS User’s Manual
- [3-6] I. C. Gomes, “Neutronics Analysis”, in IFMIF-CDA Team (ed. H. Maekawa and S. Konishi), “Minutes of the Second IFMIF-CDA Design Integration Workshop May 20-25, 1996, JAERI, Tokai, Japan”, JAERI Report, JAERI-Conf 96-012 (1996), pp.288-290.
- [3-7] N. Uda, et al., J. Nucl. Sci. Technol. 38 (2001) 936.
- [3-8] ITER Material Handbook (ed. V.Barabash).
- [3-9] A. A. Tavassoli et al., Fusion Eng. and Des. 61-62 (2002) 617.

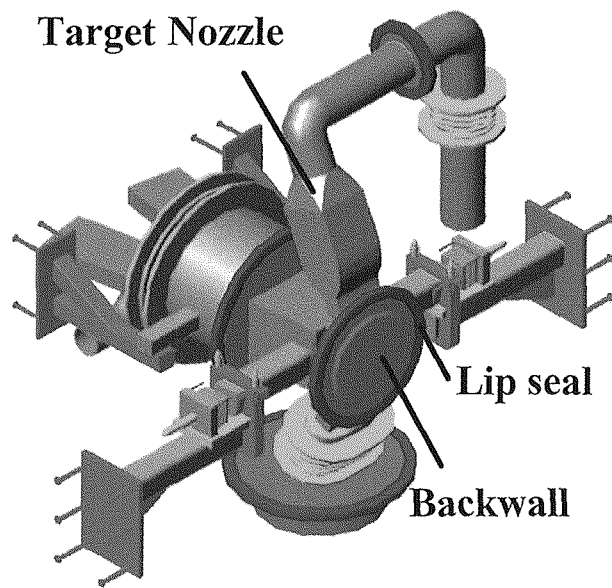


Fig. 3-1 Three Dimensional View of Target Assembly and Back-wall.

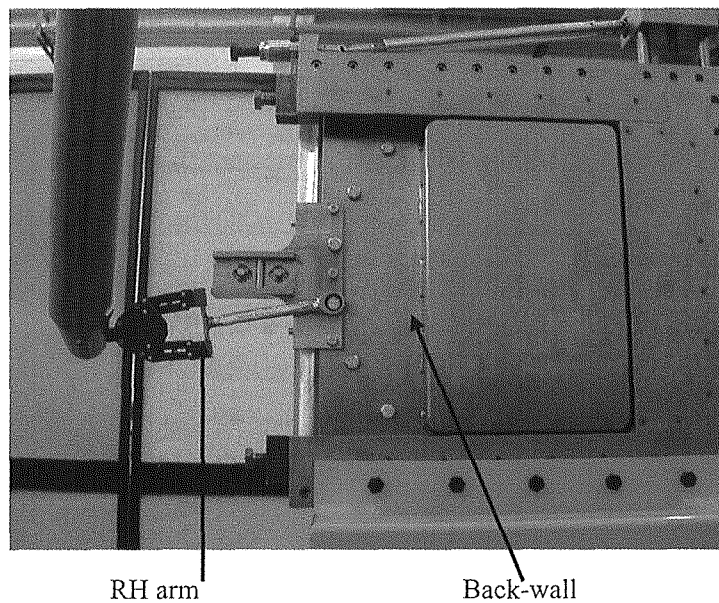


Fig. 3-2 Bayonet type mechanically replaceable back-wall.

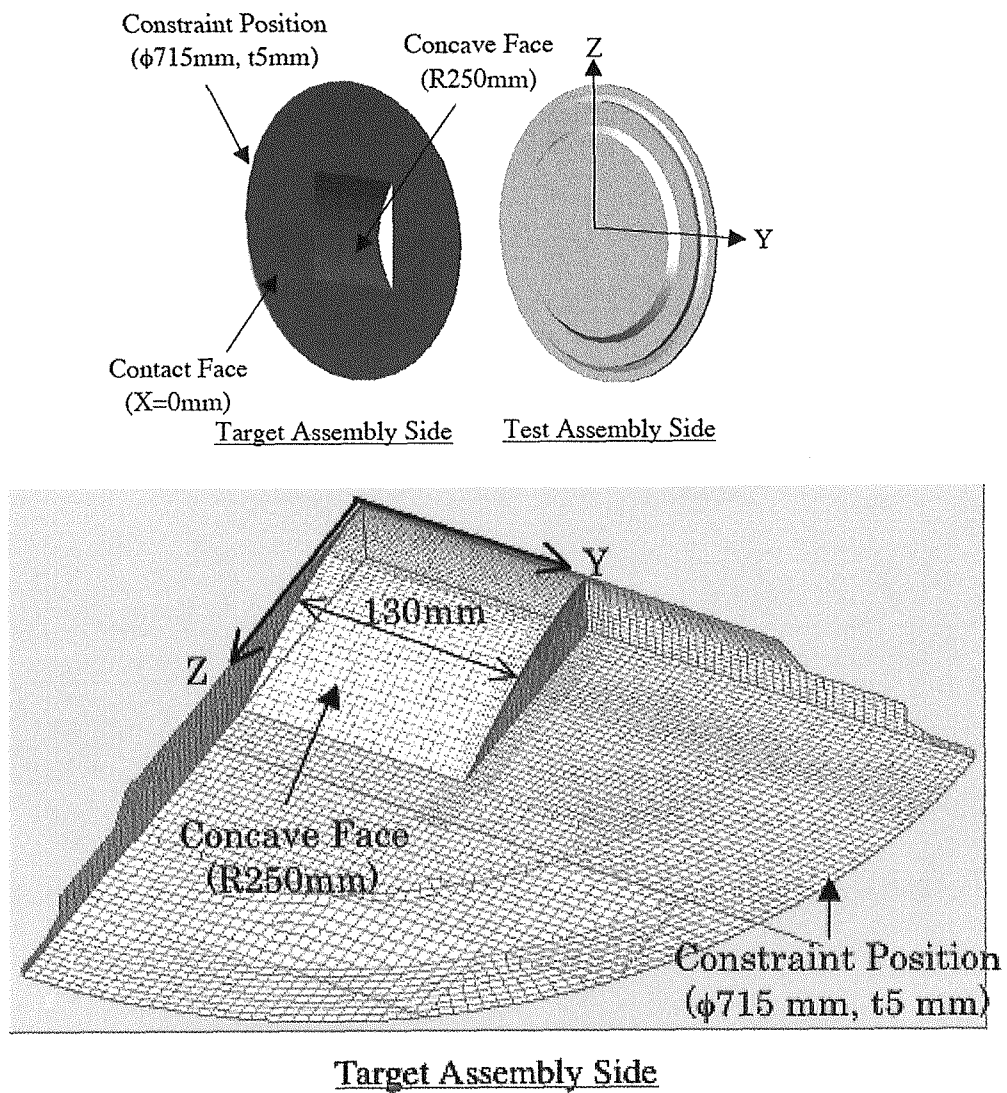


Fig. 3-3 Back-wall model for the thermal stress analysis.

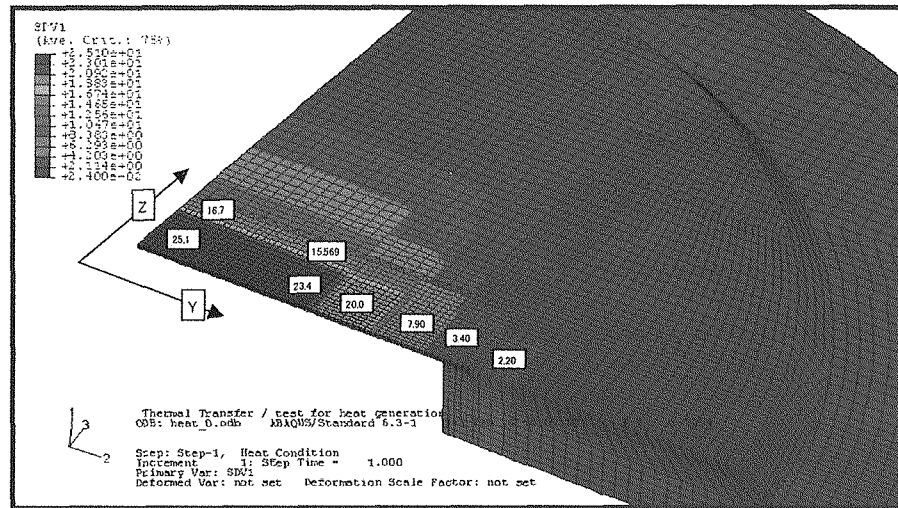
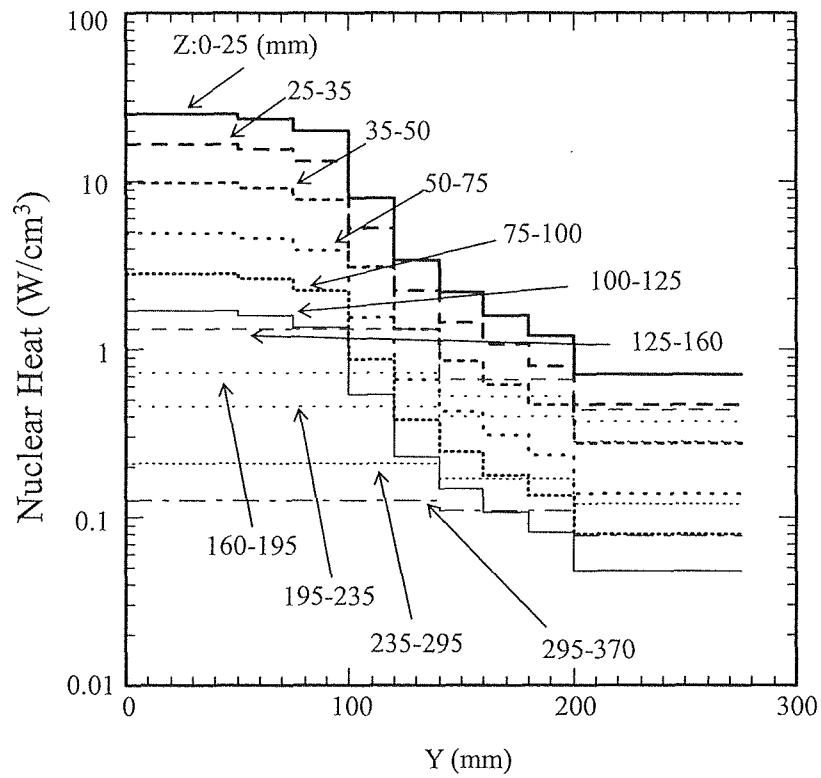


Fig. 3-4 Distribution of Nuclear Heating Rate.

Upper: Profile of nuclear heating rate,
 Lower: 2D contour of nuclear heating rate

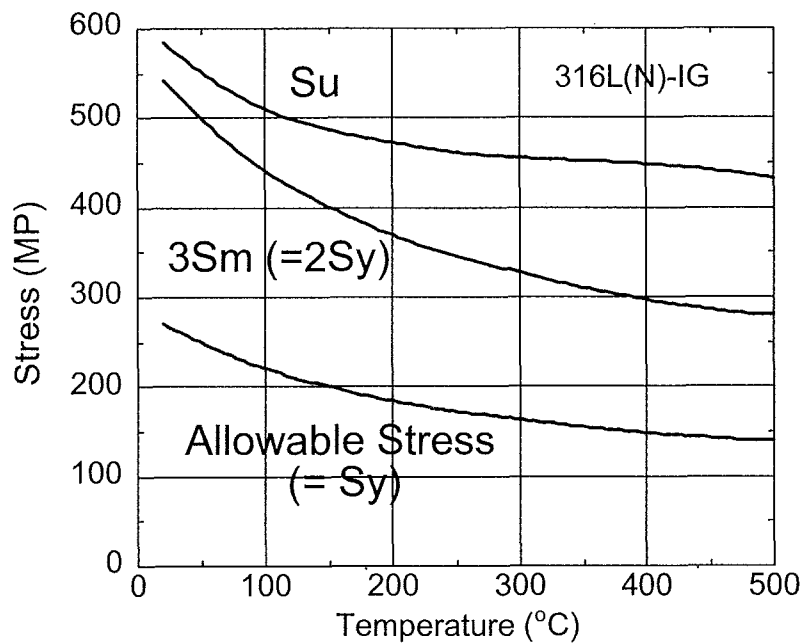


Fig. 3-5 Allowable stress of 316L(N)-IG.

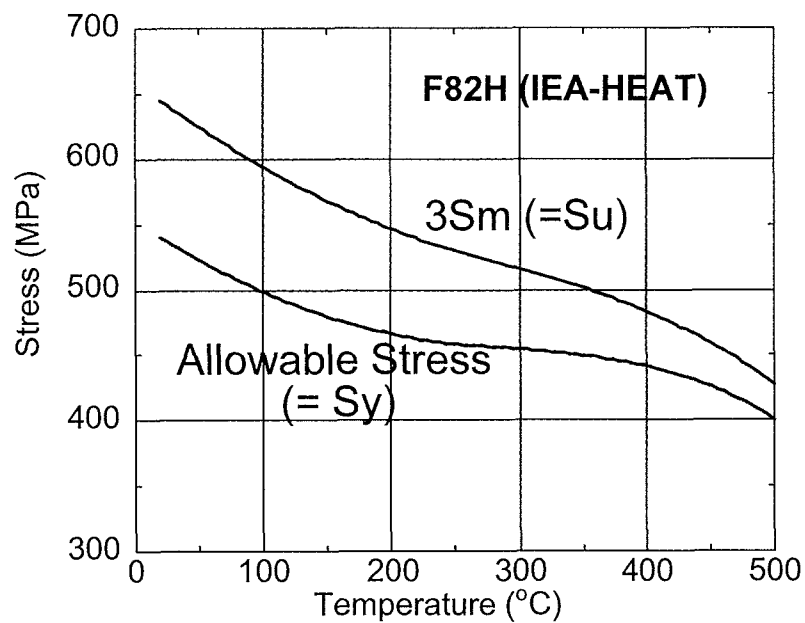


Fig. 3-6 Allowable stress of F82H (IEA-HEAT).

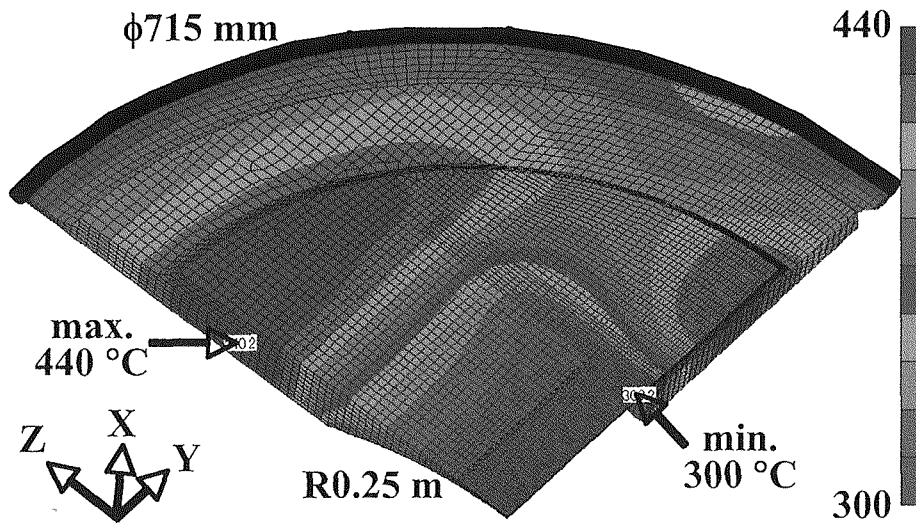


Fig. 3-7 Contour of Temperature (316L)
($t_{\min}=1.8 \text{ mm}$, $\alpha=15.8 \text{ W/m}^2\text{K}$)

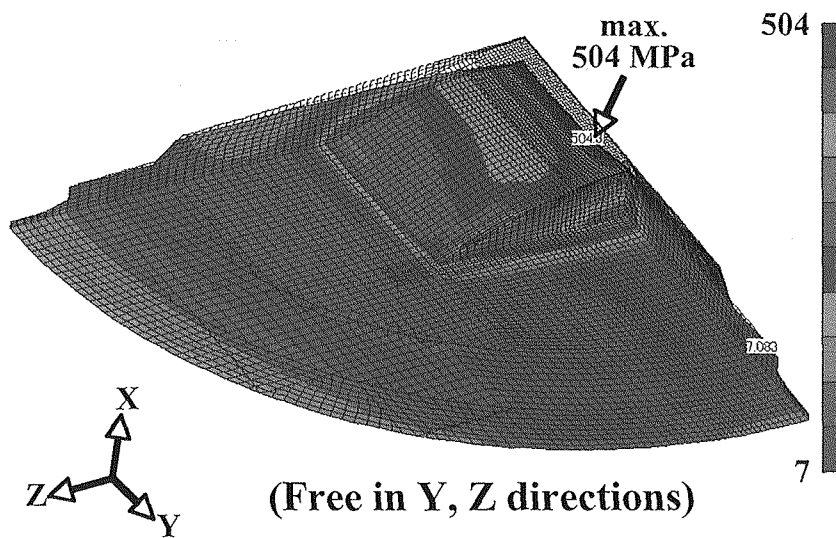


Fig. 3-8 Contour of von Mises Stress (316L)
($t_{\min}=1.8 \text{ mm}$, $\alpha=15.8 \text{ W/m}^2\text{K}$)

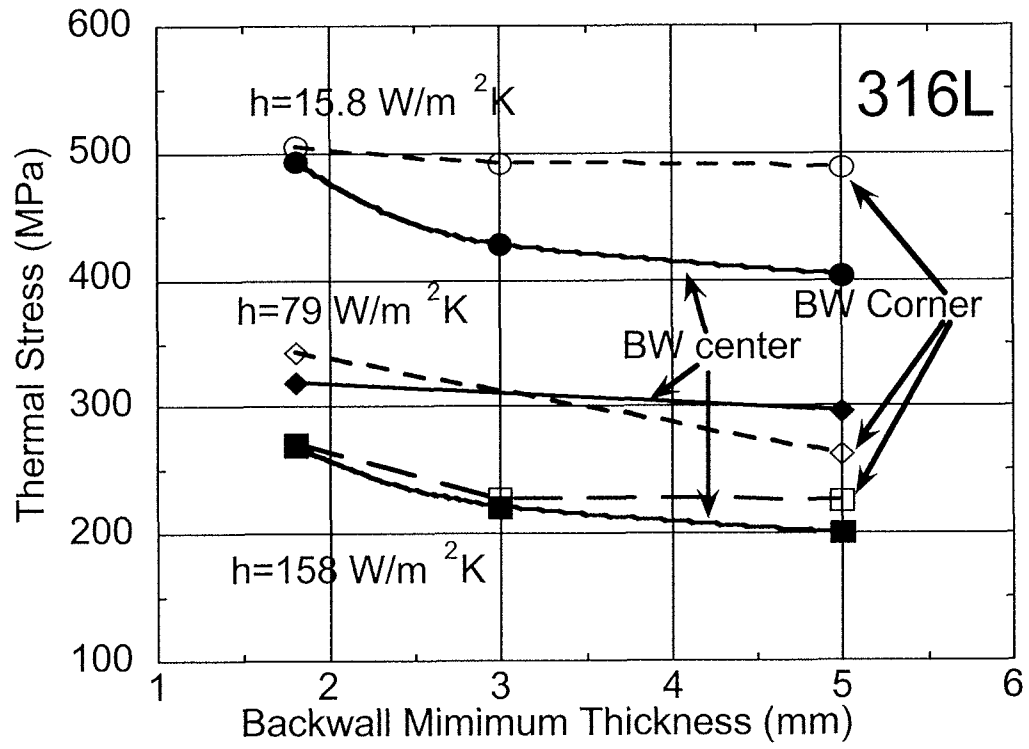


Fig. 3-9 Dependence of the backwall minimum thickness on the thermal stress of 316L back-wall.

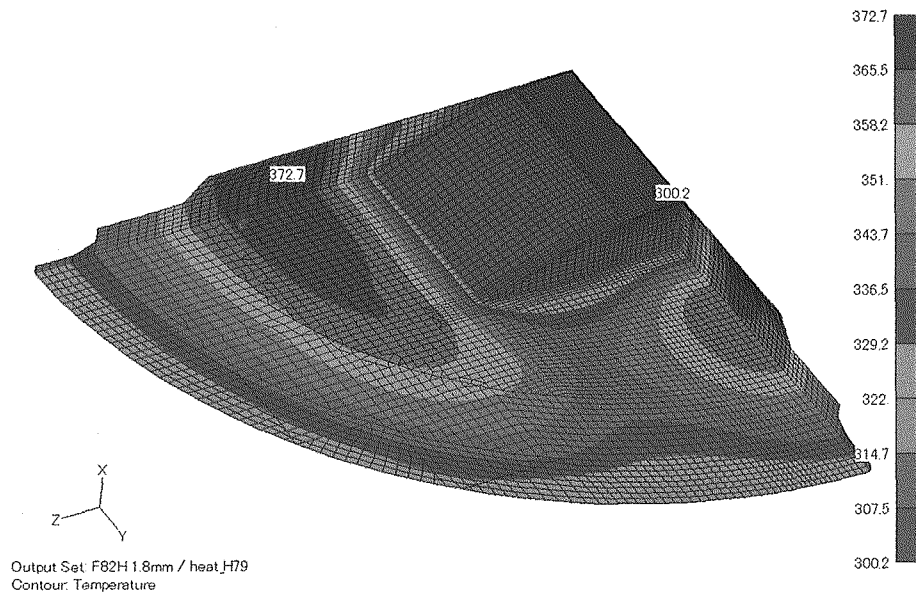


Fig. 3-10 Contour of Temperature from Li flow side view.
(F82H, $t_{\min}=1.8$ mm, $\alpha=15.8$ W/m²K)

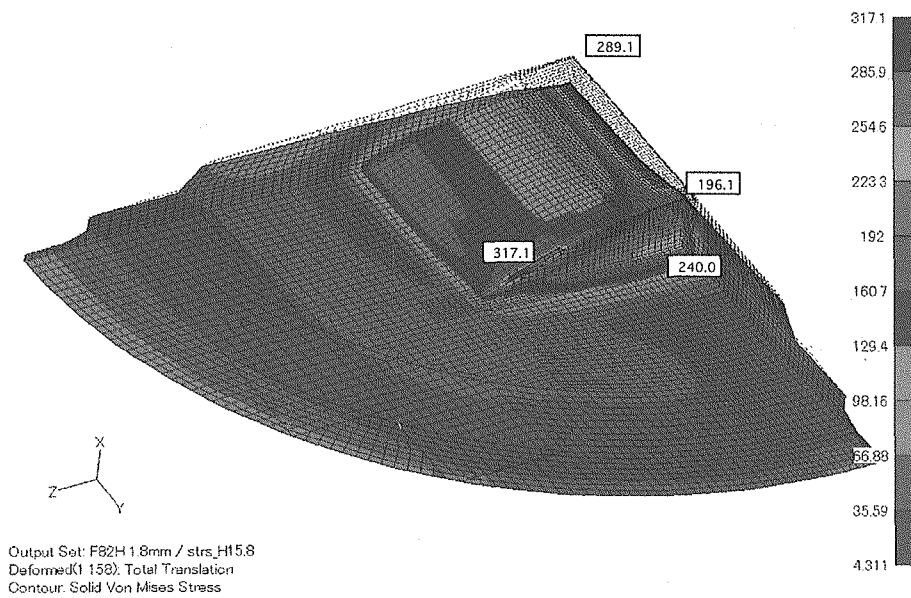


Fig. 3-11 Contour of von Mises Stress from Li flow side view.
(F82H, $t_{\min}=1.8$ mm, $\alpha=15.8$ W/m²K)

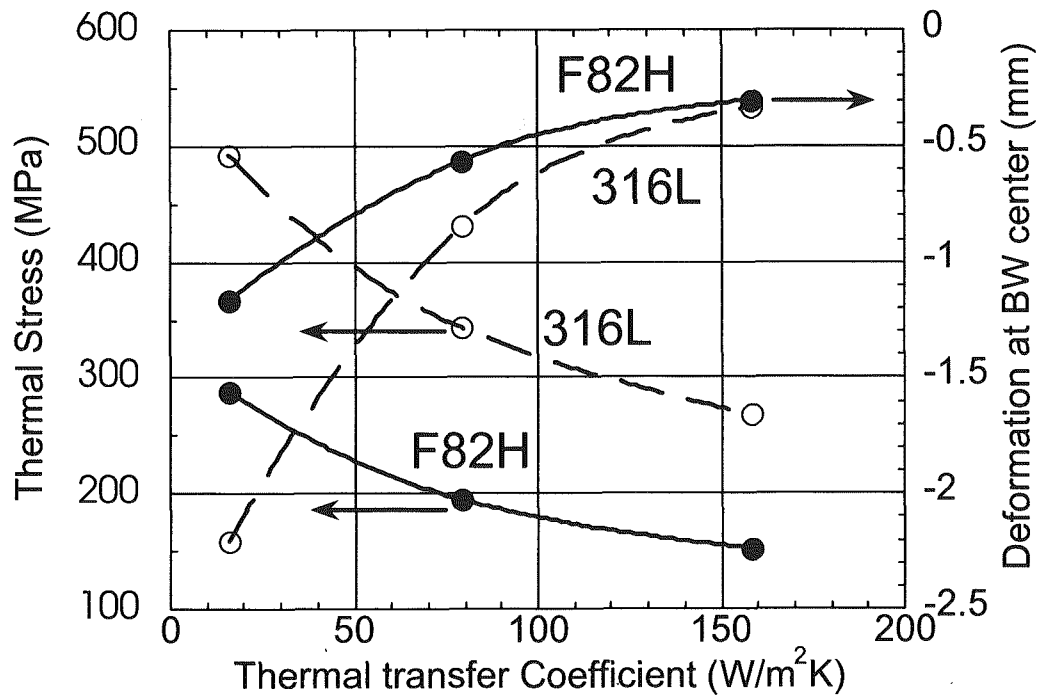


Fig. 3-12 Dependence of thermal transfer coefficient on von Mises stress and deformation of the 316L and F82H back-walls with a minimum thickness of 1.8 mm.

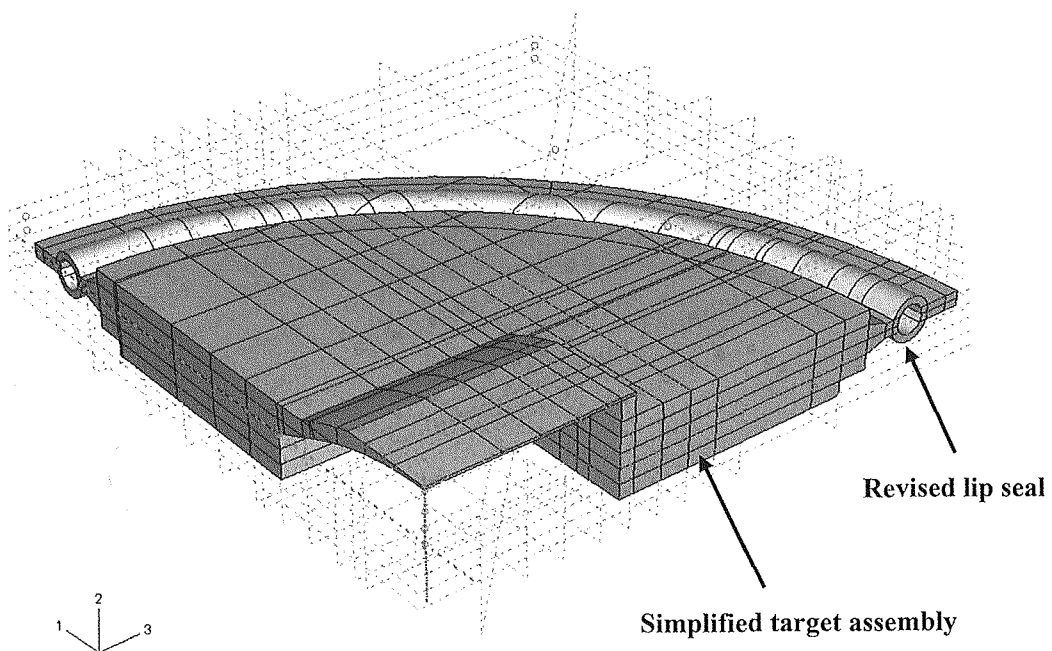


Fig. 3-13 Revised Model of the back-wall with a simplified target assembly and revised lip seal (F82H).

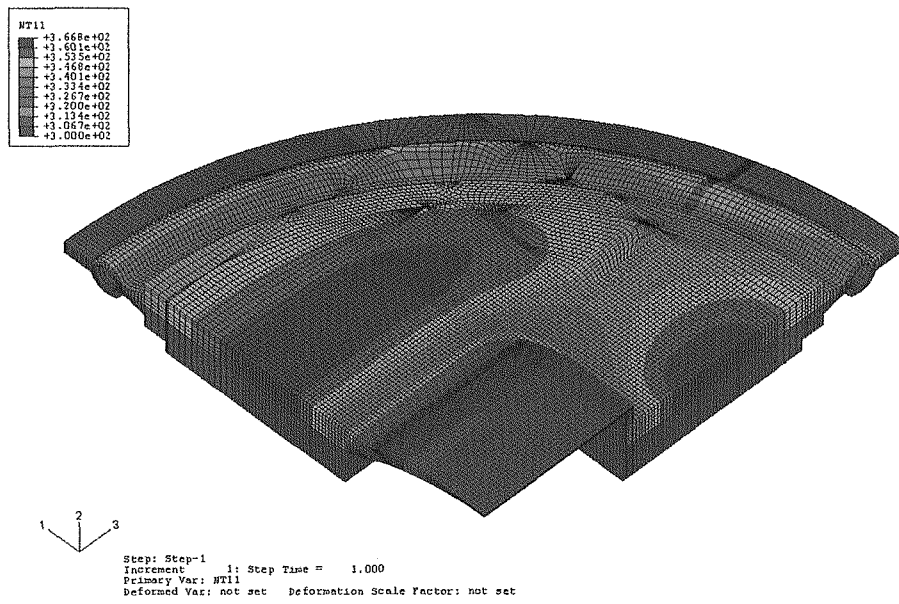


Fig. 3-14 Contour of temperature of the revised back-wall model.

(Back-wall material : F82H, $\alpha=15.8 \text{ W/m}^2\text{K}$)

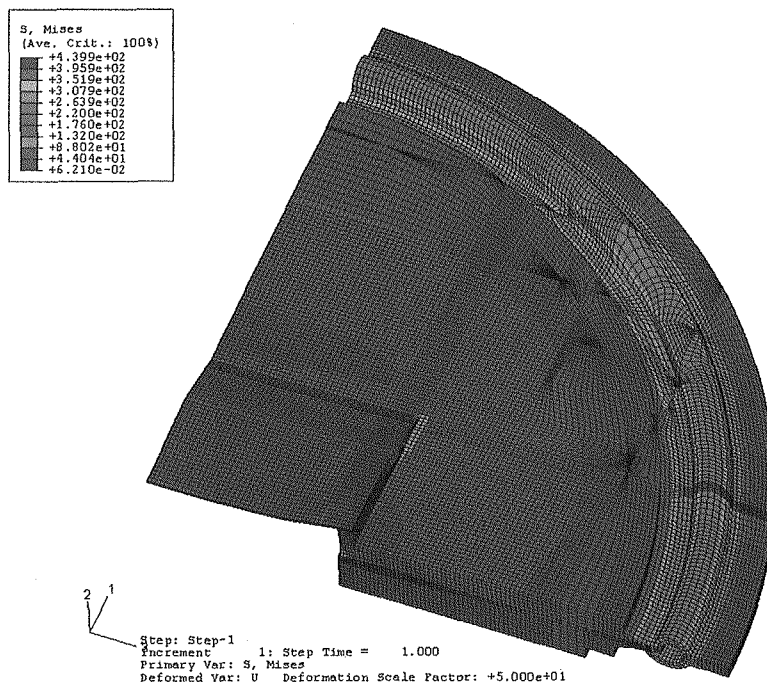
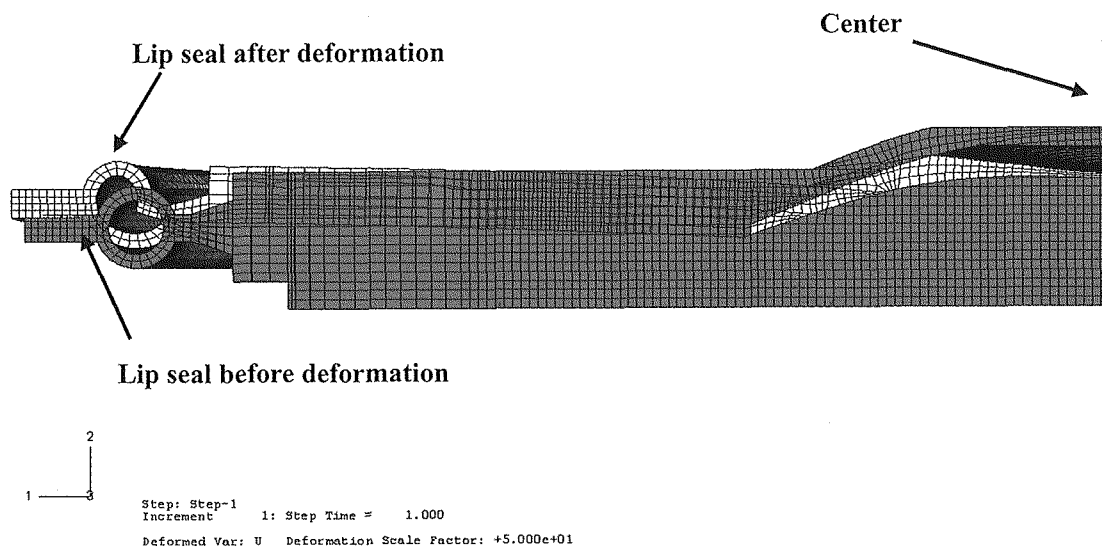


Fig. 3-15 Contour of von Mises Stress of the revised back-wall model.

(Back-wall material : F82H, $\alpha=15.8 \text{ W/m}^2\text{K}$)



**Fig. 3-16 Deformation of the revised back-wall model.
(Back-wall material : F82H)**

4. Radiation Dose Rate Due to Beryllium-7

For the IFMIF target facility, an annual maintenance after every 11-months operation is scheduled. Radioactivity in the lithium loop and required duration at the maintenance influence worker safety and system availability respectively. Beryllium-7 (^7Be) produced through the reactions $^7\text{Li}(\text{D},2\text{n})^7\text{Be}$ and $^6\text{Li}(\text{D},\text{n})^7\text{Be}$ is a dominant radioactive nuclide for worker dose in IFMIF, because its production rate is 5.02×10^{15} Be/s, using a production ratio of ^7Be to 40 MeV deuteron (D) $0.00322 (\pm 12 \%) \text{ Be/D}$ [4.1], and it emits a 0.478 MeV γ -ray with a probability of 0.105. An analytical estimation of accessibility to typical components of the IFMIF lithium loop was performed as follows.

4.1 Calculation Condition

Radioactivity of each component was assumed to be proportional to its surface area wetted by the liquid lithium as shown in Table 4-1. With a half-life of 53.3 days, a radioactivity of ^7Be can be considered to reach to almost equilibrium condition of 5.02×10^{15} Bq within IFMIF operation. In the conservative case, 100 % of the ^7Be (5.02×10^{15} Bq) deposits on inner wall of each component. A ratio of this ^7Be to lithium inventory of 4.5 t is about 80 appb and 80 wppb. Some part of the ^7Be would deposit in the cold trap in a form of $^7\text{Be}_3\text{N}_2$ with solubility of 0.5 appb [4.2] depending on conditions of temperature and nitrogen concentration. In this analysis, also deposition of 10 % of the ^7Be (5.02×10^{14} Bq) was assumed with 90 % removal performance of the cold trap.

Table 4-1 Radioactive source in component and dimension of most-outer wall of component.

Component	Length (m)	I.D. (m)	Thickness (mm)	Wet Area (m ²)	Radioactivity (Bq)	
					100% deposition	10% deposition
Pipe	6.5	0.1999	0.82	4.1	3.17×10^{13}	3.17×10^{12}
Quench Tank	2.095	1.2	12.0	9.0	7.01×10^{13}	7.01×10^{12}
EMP	2.9	0.4778	15.1	9.7	7.56×10^{13}	7.56×10^{12}
HX	7.9	1.1	15.0	576.4	4.48×10^{15}	4.48×10^{14}
Others	-	-	-	47.3	3.63×10^{14}	$4.55 \times 10^{15} *$
Total	-	-	-	646.5	5.02×10^{15}	5.02×10^{15}

* In case of 10 % deposition, most of Be-7 was assumed to exist in the cold trap.

Typical components dealt with in this analysis were a 6.5 m-long pipe the longest among the main loop, a quench tank, an electro-magnetic pump (EMP) in the main loop and a heat exchanger (HX) between the primary lithium loop and the secondary organic-oil loop. The largest source component is HX with the largest wet area 647 m² due to 434 sets of U-tube. In case of the pipe and the quench tank, their radioactivity was assumed to deposit on their cylindrical wet surfaces with "I.D." (inner diameter) shown in Table 4-1. The main EMP in the IFMIF lithium loop is that of center-return type having three cylindrical wet surfaces with diameters of 199.9 mm, 390.6 mm and 477.8 mm respectively. In case of the EMP, its

radioactivity was assumed to uniformly deposit on these three surfaces. For the HX, its radioactivity of 4.48×10^{15} Bq (4.48×10^{14} Bq in case of 10 % deposition) was assumed to uniformly deposit in the volume with length of 7.9 m and diameter of 1.1 m.

A code QAD-CGGP2R was employed to deal with three-dimensional (3-D) problem for radioactive source deposited on each component wall, buildup factor within each component wall and estimation points (virtual-detector locations). This code was revised from QAD-CGGP2 [4.3] to deal with dose equivalent rate. Cylindrical layers of the radioactive source were divided into twenty-four (in cases of the pipe and the EMP) or ninety-six (the quench tank) elements in circumference direction (θ) and more than ninety elements in length (L). In case of the HX, its volumetric source was divided into ninety-six elements in θ , ninety-eight in L and fifty-five in radial direction (R). Each small radioactive source is assumed to be a point source by the code, which calculates dose equivalent rate as sum of those due to the point sources. This discrete method caused estimation error less than 10 % (at a location 1 cm from each component wall) and less than 1 % (5 cm) in dose equivalent rate. (compare Appendixes 4-1 and 4-2)

All component walls were assumed to be made of 316L stainless steel consisting of Fe (66 %), Cr (16), Ni (12), Mn (2), Mo (2), Si (1) and void (1) in the calculation model. The atomic number and the partial density influence buildup factor and shielding performance of each element. Only the most-outer walls with "Thickness" shown in Table 4-1 were assumed for calculation of γ -ray attenuation and buildup, while the EMP has the inner cylinders and the HX has the many U-tubes. Existence of liquid lithium in the component was also ignored. These assumptions bring slightly conservative results.

4.2 Results

Figure 4-1 shows calculated results of dose equivalent rate (H) around the pipe, the quench tank, the EMP and the HX, just after shutdown of D-beam injection in the case of 100 % deposition. The rates at 1 cm distant from each component are respectively 6.5×10^5 , 5.7×10^5 , 1.1×10^6 and 1.1×10^7 $\mu\text{Sv/h}$. The maximum value is given near the HX with wet-surface area of 576 m^2 , which corresponds to 89 % of wet area in the IFMIF lithium loop. In case of the of 10 % deposition, each dose equivalent rate is 1/10 of that in the case of 100 % deposition. Any rate is far larger than the acceptable dose equivalent rate $10 \mu\text{Sv/h}$ derived from an ICRP-60 recommendation (100 mSv during 5-years) and assumed working time of 10000 hours. Access control even with distance (R) of 5 m from centerlines of component can reduce the rates only by one or two orders. Especially, in case of long component such as 7.9 m-long HX, the rate reduces almost in inverse proportion to the distance ($H \propto R^{-1}$). The rates are 6.2×10^3 , 1.2×10^4 , 1.3×10^4 and $7.2 \times 10^5 \mu\text{Sv/h}$ at the locations $R = 5 \text{ m}$ from each centerline of the pipe, the quench tank, the EMP and the HX, respectively in the case of 100 % deposition. Furthermore, even a cooling time of 1-month during annual maintenance can reduce the rates only by 1/1.5, considering the half-life of beryllium-7 53.3 days. The rate is still large, for example $4.9 \times 10^5 \mu\text{Sv/h}$ at 5 m from the HX at 30 days after a beam-shutdown. Under these conditions, no worker can carry out maintenance work such as repair and replace of component.

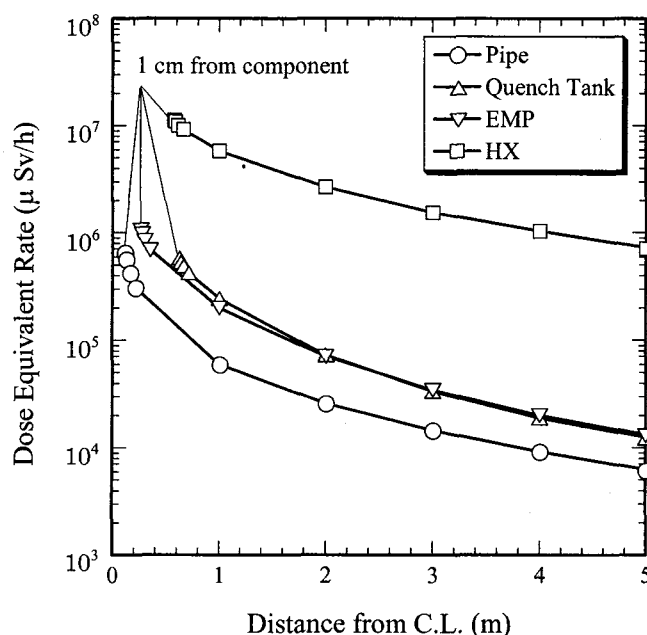


Fig. 4-1 Dose equivalent rate around each component (100 % deposition).

To reduce significant worker mentioned above, effect of radiation shielding was estimated. Iron (Fe) and lead (Pb) are candidate materials of radiation shield to attenuate γ -ray with energy of 0.478 MeV emitted from beryllium-7. An additional analysis using QAD-CGPP2R was performed to found thickness of iron/lead shield to satisfy the acceptable dose equivalent rate 10 μ Sv/h. In the code, attenuation factor is 8.46×10^{-3} and $1.62 \times 10^{-2} \text{ m}^2/\text{kg}$ respectively for iron and lead in case of γ -ray with energy of 0.478 MeV. Inputted densities of iron and lead were respectively 7.86×10^3 and $1.134 \times 10^4 \text{ kg/m}^3$. Figure 4-2 shows calculated results of dose equivalent rate around the HX without radiation shield, with iron-shield and with lead-shield, just after a beam-shutdown in the case of 100 % deposition. With attaching a 22 cm-thick iron shield or a 6.5 cm-thick lead shield to the HX, the rate can be reduced to the acceptable level less than 10 μ Sv/h. The rates are 9.3 and 9.7 μ Sv/h at locations 1 cm from the iron and the lead shield respectively. The rate reduces in inverse proportion to the distance ($H \propto R^{-1}$) in a region $R > 1 \text{ m}$, and thus the rate beyond the calculation region ($R > 5 \text{ m}$) can be predicted.

Mass of the shield is 57 t (the 22 cm-thick iron shield) and 22 t (the 6.5 cm-thick lead shield). Any of them is larger than that of HX 19 t. In case that these heavy shields are not acceptable from viewpoint of rational design of the target system, other measures for worker safety should be investigated. Possible measures are employments of a cold trap and remote-handling system. Figure 4-3 shows calculated results in the case of 10 % deposition assuming impurity removal by a cold trap. Needed thickness of the shield reduces to 18.4 and 5.3 cm respectively for iron and lead shields. More estimation on beryllium-7 localization in a cold trap under temperature gradient condition is needed. Also investigation of remote-handling system suffering γ -ray corresponding to $10^7 \mu\text{Sv/h}$ is needed. These tasks for design of the target system are to be carried out in IFMIF Engineering Validation and Engineering Design Activity.

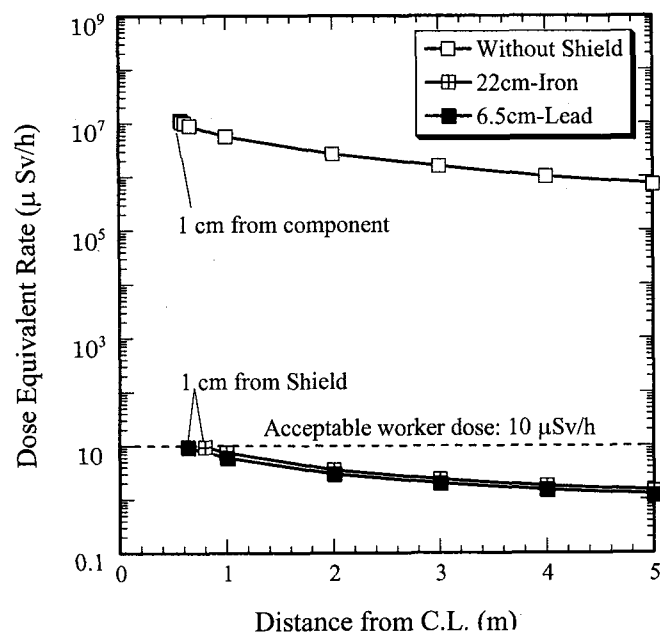


Fig. 4-2 Dose equivalent rate around shielded heat exchanger (100 % deposition).

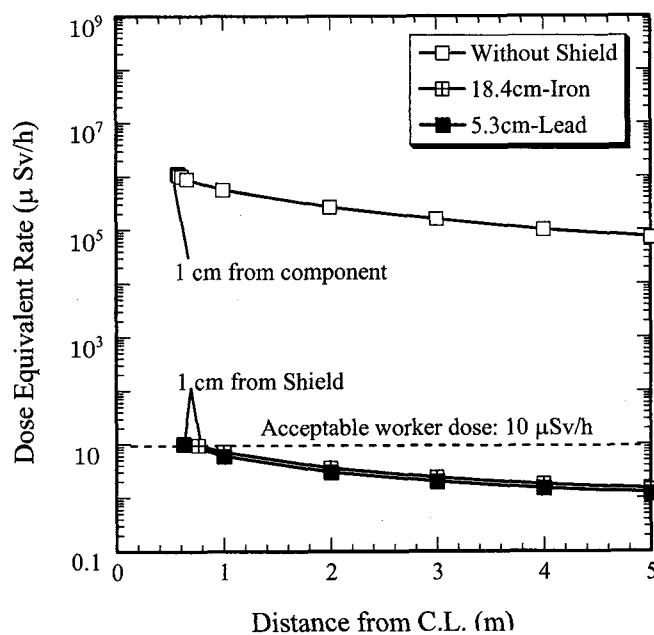


Fig. 4-3 Dose equivalent rate around shielded heat exchanger (10 % deposition).

4.3 Summary

Dose equivalent rate around typical component in the IFMIF lithium loop was several orders higher than the acceptable level of $10 \mu\text{Sv/h}$. In the most conservative case assuming 100 % deposition of beryllium-7, maximum value was $1.1 \times 10^7 \mu\text{Sv/h}$ at a location 1 cm from the heat exchanger due to its large wet-surface area of 576 m^2 .

The dose equivalent rate around the heat exchanger can be reduced by 22 cm-thick iron-shield or 6.5 cm-thick lead-shield to the acceptable level.

Employment of a cold trap reduces the dose equivalent rate and needed thickness of the radiation shield. For example, the shield thickness was 18.4 and 5.3 cm respectively for iron and lead shields in the case of 10 % deposition.

References

- [4.1] U. von Möllendorff, F. Maekawa, H. Giese and H. Feuerstein, "A nuclear simulation experiment for the International Fusion Materials Irradiation Facility (IFMIF)", FZK report FZKA 6764, 2002.
- [4.2] IFMIF Team (ed. A. Möslang), "IFMIF International Fusion Materials Irradiation Facility Conceptual Design Evaluation Report A Supplement to the CDA by the IFMIF TEAM", FZK report FZKA 6199, 1999.
- [4.3] Y. Sakamoto and S. Tanaka, "QAD-CGGP2 and G33-GP2: Revised versions of QAD-CGGP2R and G33-GP", JAERI report JAERI-M 90-110, 1999.

5. Summary

Dose equivalent rate around typical component in the IFMIF lithium loop was several orders higher than the acceptable level of $10 \mu\text{Sv/h}$. In the most conservative case assuming 100 % deposition of beryllium-7, maximum value was $1.1 \times 10^7 \mu\text{Sv/h}$ at a location 1 cm from the heat exchanger due to its large wet-surface area of 576 m^2 . The dose equivalent rate around the heat exchanger can be reduced by 22 cm-thick iron-shield or 6.5 cm-thick lead-shield to the acceptable level. Employment of a cold trap reduces the dose equivalent rate and needed thickness of the radiation shield. For example, the shield thickness was 18.4 and 5.3 cm respectively for iron and lead shields in the case of 10 % deposition.

Thermo-structural analyses of the "Cut and reweld" type replaceable back-wall made of 316L stainless steel and F82H have been done by ABAQUS code. In a case of the 316 stainless steel back-wall, the von Mises stress was higher than a permissible value of 140 MPa at 300 °C. However, in a case of F82H back-wall, the von Mises stress is less than a permissible value of 455 MPa at 300 °C. Therefore, F82H is recommended as a back-wall material. In case of the revised model with a simplified target assembly and the lip seal, the thermal stress and the deformation at the back-wall center are significantly reduced. However, in this case, the maximum thermal stress is observed at the lip seal.

In future, engineering design and validation of the target system will be done in the EVEDA.

Acknowledgements

Appreciation is given to all members of the IFMIF international team on their contributions to this work. The IFMIF executive subcommittee has been highly impressed with dedication and enthusiasm of the IFMIF team. Also, appreciation is given to for the continued interest of the IEA Fusion Power Coordinating Committee and IEA Executive Committee on Fusion Material. Finally, the authors in JAEA are grateful to Drs. M. Seki, S. Seki and H. Takatsu for their supports to IFMIF activities.

Appendix 4-1. Dose equivalent rate H_C around each component without shield (100% deposition). (unit: $\mu\text{Sv/h}$)

Component	R	$R_W + 1 \text{ cm}$	$R_W + 2 \text{ cm}$	$R_W + 5 \text{ cm}$	$R_W + 10 \text{ cm}$	1 m	2 m	3 m	4 m	5 m
Pipe (6.5 m)		6.467E+05	5.628E+05	4.231E+05	3.067E+05	5.895E+04	2.565E+04	1.438E+04	9.083E+03	6.203E+03
Quench Tank		5.744E+05	5.392E+05	4.841E+05	4.227E+05	2.471E+05	7.311E+04	3.336E+04	1.891E+04	1.214E+04
EMP		1.061E+06	9.739E+05	8.331E+05	6.892E+05	2.012E+05	7.070E+04	3.459E+04	2.020E+04	1.317E+04
HX		1.110E+07	1.083E+07	1.012E+07	9.158E+06	5.741E+06	2.634E+06	1.562E+06	1.025E+06	7.182E+05

H_C : Dose equivalent rate $H(R, L, \theta)$ at mesh center $L = \Delta L/2$, $\theta = \Delta\theta/2$ resulting in rater large values near the components

R_W : R at outside of most-outer wall of each component

Appendix 4-2. Dose equivalent rate H_B around each component without shield (100% deposition). (unit: $\mu\text{Sv/h}$)

Component	R	$R_W + 1 \text{ cm}$	$R_W + 2 \text{ cm}$	$R_W + 5 \text{ cm}$	$R_W + 10 \text{ cm}$	1 m	2 m	3 m	4 m	5 m
Pipe (6.5 m)		6.349E+05	5.605E+05	4.227E+05	3.071E+05	5.890E+04	2.566E+04	1.439E+04	9.094E+03	6.211E+03
Quench Tank		5.449E+05	5.338E+05	4.840E+05	4.227E+05	2.471E+05	7.311E+04	3.336E+04	1.891E+04	1.214E+04
EMP		9.708E+05	9.430E+05	8.306E+05	6.894E+05	2.013E+05	7.065E+04	3.458E+04	2.020E+04	1.317E+04
HX		1.110E+07	1.083E+07	1.012E+07	9.158E+06	5.741E+06	2.634E+06	1.562E+06	1.025E+06	7.182E+05

H_B : Dose equivalent rate $H(R, L, \theta)$ at mesh boundary $L = 0$, $\theta = 0$ resulting in rater small values near the components

Appendix 4-3. Dose equivalent rate \dot{H}_C around heat exchanger. (unit: $\mu\text{Sv/h}$)

Condition	R	R _{W/S} + 1 cm	1 m	2 m	3 m	4 m	5 m
HX (100% deposition) without shield		1.110E+07	5.741E+06	2.634E+06	1.562E+06	1.025E+06	7.182E+05
HX (100% deposition) + 22 cm-Iron		9.321E+00	7.362E+00	3.651E+00	2.430E+00	1.822E+00	1.453E+00
HX (100% deposition) + 6.5 cm-Lead		9.687E+00	6.106E+00	3.030E+00	2.017E+00	1.512E+00	1.203E+00
HX (10% deposition) without shield		1.110E+06	5.741E+05	2.634E+05	1.562E+05	1.025E+05	7.182E+04
HX (10% deposition) + 18.4 cm-Iron		9.488E+00	7.136E+00	3.536E+00	2.354E+00	1.763E+00	1.402E+00
HX (10% deposition) + 5.3 cm-Lead		9.860E+00	6.077E+00	3.013E+00	2.006E+00	1.501E+00	1.190E+00

R_{W/S}: R at outside of most-outer wall/shield of each component